20

Near-Field Scanning Optical Microscopy for Bioanalysis at Nanometer Resolution

Musundi B. Wabuyele, Mustafa Culha, Guy D. Griffin, Pierre M. Viallet, and Tuan Vo-Dinh

Summary

The nondestructive imaging of biomolecules in nanometer domains in their original location and position as adsorbed or deposited on a surface is of garners considerable experimental interest. Near-field scanning optical microscopy (NSOM) is an emerging technique with its astonishing resolving power of <100-nm domains, and nondestructive nature compared with other scanning probe microscopic techniques is an emerging technique to achieve this goal. At the single-molecule level of resolution, it is possible to use the NSOM as a critical tool for visualization of proteins on surfaces to obtain more fundamental information about their orientation and locality without disturbing their original orientation and position, and level of interaction with the surface. Several areas of science and medicine can benefit from this type of study especially for biomedical and biochip applications. To illustrate possible applications, imaging of green fluorescent proteins and biomolecules associated with multidrug resistance proteins in tumor cells will be demonstrated using NSOM.

Key Words: Near-field scanning optical microscopy; protein; biomolecules; multidrug resistance transport protein; P-glycoprotein.

1. Introduction

Optical microscopy is an important technology that finds applications in scientific and technological arenas ranging from imaging of living specimens and characterization of advanced materials to the spectroscopic analysis of semiconductors. There is an increasing demand for higher spatial resolution to obtain more information about the given area of a sample or a molecule on a surface or in a cell. Disappointingly, conventional optics limits the resolution as determined by Abbé ***(1)***, to λ/2 or 200 nm for visible light. In 1928, Synge ***(2)*** overcame this barrier by suggesting that light exciting an aperture is

From: *Methods in Molecular Biology, vol. 300: Protein Nanotechnology, Protocols, Instrumentation, and Applications*
Edited by: T. Vo-Dinh © Humana Press Inc., Totowa, NJ

confined to roughly the dimensions of an aperture having subwavelength dimensions. Even though this principle was the first demonstrated in the microwave region of the spectrum in 1972 ***(3)***, it could be applied at optical wavelengths with the design and introduction of subwavelength aperture optical probes. Near-field scanning optical microscopy (NSOM) not only overcomes the diffraction limitation of conventional optics but also combines the enhanced lateral and vertical resolution allowing the use of characteristic scanning probe microscopies with simultaneous measurements of topographical and optical signals.

Scanning probe microscopy (SPM) was revolutionized by the development of high-resolution techniques such as scanning force microscopy (AFM) and scanning tunneling microscopy (STM). A high resolution of images of biological samples such as cells or DNA has been successfully demonstrated using AFM at a molecular level. However, only topographical information can be obtained because AFM acquires images based on the force interaction between the tip and the surface of the sample. Alternatively, samples for STM must be conductive. In contrast, NSOM probes do not come in contact with the sample; hence, it is noninvasive in nature and does not perturb the sample (*see* **Fig. 1**) ***(4)***. NSOM combines enhanced lateral and vertical resolution and has the ability to attain spatial resolution approaching nanometer scale. This is an apparent advantage over other scanning and optical techniques and can help researchers to understand phenomena is challenged by several areas of science including nanotechnology, biomaterial science, and biosciences.

NSOM is based on scanning a very small light source with dimensions smaller than its wavelength very close (in the near field) to the sample. The light source is a tapered optical fiber from one end and coated with aluminum on its outside walls. The light that is coupled to the fiber is radiated from the tapered and aluminum-coated end. This emanated light passes through an aperture (approx 50 to 100 nm) with an exponential attenuation away from the tip. As shown in **Fig. 2**, near-field illumination of the sample at a distance h_1 less than the wavelength (λ) of incident light gives high-resolution images compared with those obtained from far-field illumination in which the distance $h_2 >> \lambda$ and greater than the aperture. Thus, subwavelength details of the image are lost.

Over the past decade, NSOM has evolved into a new frontier in science ***(5)*** with a high impact and potential in various areas of research ranging from biomedical to analytical to biological sciences. Betzig and Chichesterd were among the first pioneers to investigate biological tissues using NSOM ***(6)***. Thin-tissue sections of the hippocampus region of monkey brain were imaged using NSOM. Other experiments have been performed in an attempt to distinguish single actin filaments in the cytoskeleton. The actin filaments were stained selectively with rhodamine-labeled phalloidin and imaged with NSOM

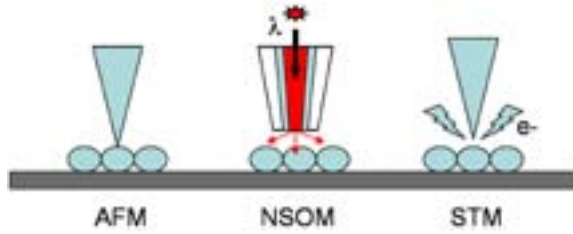

Fig. 1. Comparison of SPMs. AFM involves a cantilever being scanned over the surface of a sample. The measured cantilever deflections are used to generate topographical images. NSOM involves a tapered optical fiber probe coupled to a laser light and is used to excite fluorophores as the probe is scanned over the surface of a sample. STM uses a sharpened conducting tip with a bias voltage applied between the tip and the sample. When the tip is brought within about 10Å of the sample, electrons ($\mathbf{e}^-$) from the sample begin to "tunnel" through the gap into the tip. The resulting tunneling current varies with tip-to-sample spacing, and it is the signal used to create an STM image.

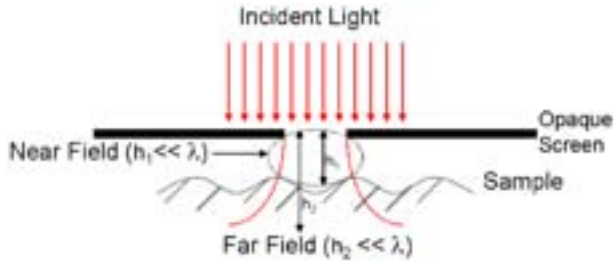

Fig. 2. Principles of NSOM. A subwavelength-size aperture confines the laser light and illuminates the sample in close proximity (typically <10 nm) with a depth of h_1 (near field) and h_2 (far field).

(7,8). Moers et al. ***(9)*** studied fluorescently labeled chromosomes by combining cytochemical and scanning probe techniques, which enabled the localization and identification of several fluorescently labeled genomic DNA fragments on a single chromosome with extraordinary resolution. In 1998, Garcia-Parajo et al. ***(10)*** studied the photodynamics of individual fluorescence molecules, which were localized with an accuracy of 1 nm. Later, Garcia-Parajo et al. ***(11)*** reported on studies of green fluorescent protein (GFP) as an individual marker for applications in molecular biology for detailed understanding of its photophysical and photodynamic properties. They investigated both individual S65T mutants of GFP on a glass surface and embedded in a water-pore gel. Kirsch et al. ***(12)*** studied the imaging of pUC18 relaxed circular plasmid DNA

spread on mica precoated with cetylpyridinium chloride. This study demonstrated the applicability of the shear force signal (topography) in conjunction with the optical signals from fluorescence to image biological macromolecules.

Several groups have demonstrated applications of NSOM in cell biological studies. These applications include the imaging of cytoskeleton components in 3T3 fibroblasts by Betzig et al. ***(13)***, as well as membrane mapping and colocalization of malarial and host skeletal proteins in red blood cells infected with the human malaria parasite *plasmodium falciperum* ***(14)***. Other studies used NSOM to detect activation-dependent clustering of the erB2 receptor, a member of the epidermal growth factor (EGF) family that is overexpressed in breast cancer patients ***(15)***. In another study, Deckert et al. ***(16)*** combined NSOM and surface-enhanced Raman scattering (SERS) to image brilliant cresyl blue-labeled DNA on Teflon nonospheres covered with evaporated silver layers. The imaging of fluorescently labeled DNA with high spatial resolution and single-molecule fluorescence sensitivity was demonstrated, and no sample deformation was observed under the reported experimental conditions ***(17)***. In another study, researchers used a planar silver island-based SERS substrate to generate SERS signals and a chemically etched, 200-nm optical fiber tip to deliver excitation radiation from an argon ion laser (488 nm). The tapered sides of the fiber tip were coated with a thick, opaque layer of metal to confine the excitation radiation to the 200-nm tip, hence permitting extremely localized sample excitation. This factor, combined with a substrate-to-fiber tip spacing of approx 0.1 nm, enabled the acquisition of spectral and spatial information, with subwavelength lateral resolution, for CFV and rhodamine 6G molecules ***(18,19)*** distributed on the silver island substrate. Furthermore, the SERS-NSOM technique demonstrated exceptional sensitivity. Spectra from as few as 300 molecules have been recorded. Schmalenberg et al. ***(20)*** studied imaging of laminin and bovine serum albumin proteins with AFM and NSOM on a patterned glass surface in both dry and hydrated environment.

The capability to generate patterned surfaces with biomolecules such as proteins for biosensor technology ***(21)***, for tissue engineering ***(22)***, and for fundamental studies of protein adsorption on surfaces for development of biocompatible materials is extremely important. As a result of extensive studies in genomics and proteomics, the biochip concept has been developed. A biochip is an array of dots, with each dot containing a small volume of proteins and fragments of DNA. In a protein biochip, the spots contain a range of proteins, and/or visualization of these proteins in their original location and position with NSOM in nanometer resolution may play a critical role in understanding their interaction with other molecules.

In the present study, we investigated the localization of multidrug resistance (MDR) transport proteins and their effect on chemotherapeutic drugs. The development of multi-drug resistance owing to expression of MDR proteins in cells has been a major hindrance to successful delivery of chemotherapeutic drugs. By this mechanism, cancer cells become resistant to many drugs of diverse structure and mechanism when exposed to this drug. Two kinds of proteins, multidrug resistance protein (MRP) and P-glycoprotein (P-gp), play a key role in the MDR phenomenon; however, their locality and mechanism of action still remain a subject of interest. In addition to the confocal microscopy and other biological techniques previously reported, we would like to apply the advantages of NSOM to determine the localization and effects of these proteins in the chemotherapeutic treatment of human cancers.

2. Materials

2.1. Cell Lines

Chinese hamster ovary (CHO) lines were obtained from the American Type Culture Collection (Manassas, VA). MTLN3 cells were kindly provided by Dr. Jeffrey E. Segall (Albert Einstein College of Medicine, Department of Anatomy and Structural Biology).

2.1.1. Cell Culture and Fixation

The cells were cultured (95% humidity, 5% CO_2, 37°C) on glass chamber slides from Nalge Nunc (Naperville, IL) in F-12 (Invitrogen, Carlsbad, CA) with 10% fetal bovine serum (FBS) (Gibco, Grand Island, NY) for CHO, and 5% FBS in Dulbecco's modified Eagle's medium (Invitrogen) with 0.5% Pen/Strep for MTLN3 cells. When the cells reached 70 to 80% confluence (3 d), they were subcultured at a 1:20 split ratio for CHO and MTLN3. The cells were fixed with 4% paraformaldehyde for 5 min followed by multiple rinses with methanol followed by 100% cold ethanol.

2.1.2. Cell Labeling With Drugs and Dyes

Yellow-green fluorescent FluoSpheres beads and BODIPY® FL verapamil hydrochlorides were purchased from Molecular Probes. Doxorubicin (DOX) was obtained from Sigma (St. Louis, MO). Cells were incubated with the indicated dyes and drugs for 2 h in their respective medium in a 5% CO_2, 37°C incubator. Prior to fixing, the cells were washed with phosphate-buffered saline buffer.

2.2. NSOM Instrumentation

1. Instrument stage (base plate with mounted hardware).
2. Aurora-2 sensor head.

3. Electronic Control Unit-*Plus* (ECU-*Plus*) with I/O 10 and I/O MOD+ boards.
4. Aurora Control Unit.
5. Computer.
6. Video monitor.
7. NSOM fiberoptic tips.
8. Probe installation tool.
9. Fiber cleaver.
10. Fiber stripper tool.
11. Tool kit.
12. NSOM standard sample.
13. User's manual.
14. SPMLab software.
15. SPMLab Software Reference Manual.
16. Laser.
17. Laser coupler.
18. Vibration isolation table.

2.2.1. Setup of System

A TopoMetrix Aurora-2 Near-field Scanning Optical Microscope was used for our experiments. The Aurora-2 instrument is a platform for obtaining topographic and optical images. A sample is mounted on an X-Y scanning stage, which is controlled by a three-piezo scanner arrangement. The fiberoptic probe is mounted on the removable Aurora-2 microscope head and positioned above the sample. Topographic and optical images can be taken simultaneously. As shown in **Fig. 3**, the sample is laterally scanned beneath the fiber tip with a distance of 5 to 10 nm being maintained by monitoring the shear-force interaction between the lateral vibrating tip and the sample surface. The scanning process is controlled by the electronics of the SPM system. The optical components of the Aurora-2 system are used for taking NSOM data as well as for focusing the optics and monitoring the probe-sample approach. The rotating mirror (*see* **Fig. 4**) selects either the reflection or transmission objective. The two "flipper" mirrors can be manually flipped down to allow use of the photomultiplier tube (PMT) or optional hardware, such as a photon counter or spectrometer.

For NSOM imaging, multiple excitation sources can be used depending on what kind of chromophore is being investigated. A 488-nm argon-ion laser equipped with laser-line filter was used as an excitation source for our experiments. The emission light was collected via the transmission mode through a ×40, 0.65N.A objective and through a set of filters, dichroic mirror (510DF10) and bandpass filter (520LP10), obtained from Omega Optical. The fluorescence signal was then detected by a PMT and analyzed with commercial software (SPMLab).

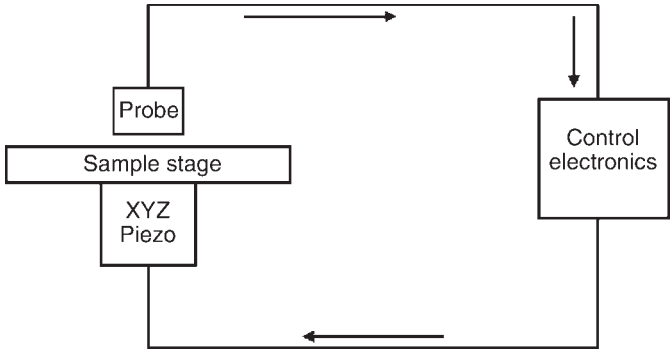

Fig. 3. Schematic layout of Aurora-2 system showing topography feedback loop. The sample is mounted on a scanning stage, which is controlled by a three-piezo scanner arrangement. The fiberoptic probe is mounted on the removable Aurora-2 microscope head and positioned above the sample.

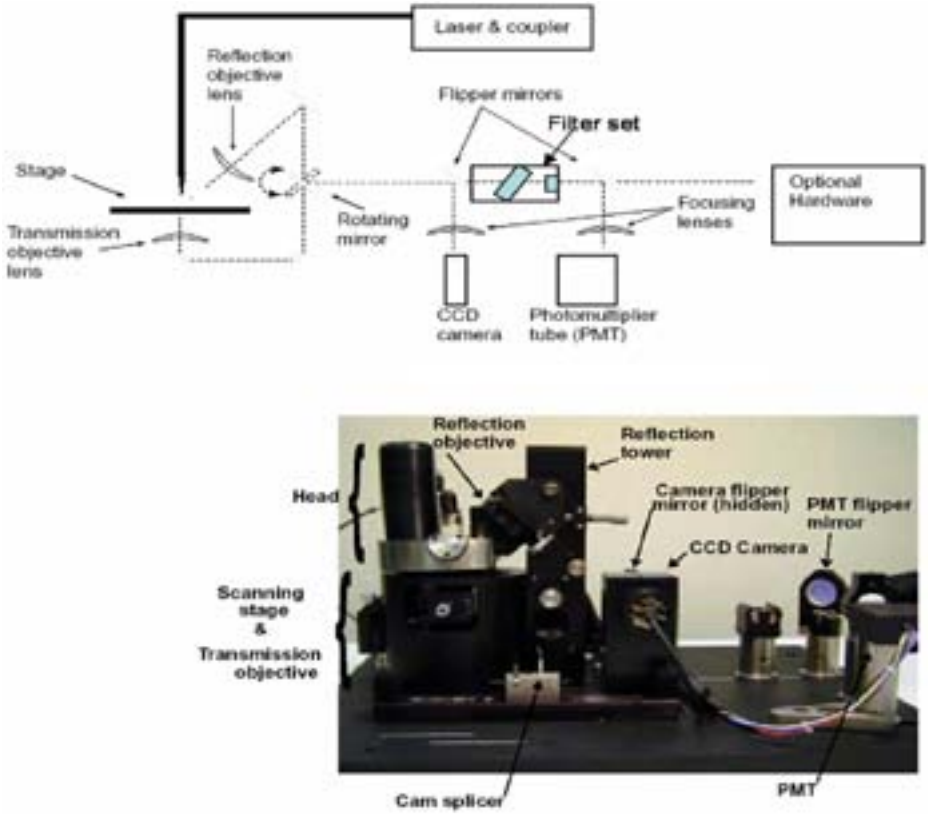

Fig. 4. Block diagram showing **(A)** light path and **(B)** components of Aurora-2 system. CCD, charge-coupled device.

3. Methods

The methods discussed next describe the sample and tip mounting, and laser coupling, as well as providing an example of the preparation of sample and experimental setup for simultaneous topographical and NSOM imaging of biomolecules in cells.

3.1. Preparation of Sample

Samples are prepared on a thin optically transparent glass substrate. Cells were cultured and fixed on glass chambers that were 200 mm thick. For good imaging, the sample has to be relatively flat. Typically, sample height features of <500 nm in size and a scan range of 30 × 30 μm is acceptable. Rough surfaces make feedback difficult because the tip is easily damaged (*see* **Note 1**).

3.2. Sample and Probe Mounting, and Laser Coupling

To mount the sample, the head must be removed and the sample slide can be simply taped to the stage (*see* **Notes 2–4**). The probe is installed to the probe cartridge with the help of a probe installation tool (*see* **Note 5**). After stripping away about 2.5 cm of the polymer buffer from the distal end of the fiber with the help of a fiber stripper tool, the end of the tip fiber is cleaved with the optical fiber cleaver (*see* **Note 6**). Finally, the fiber tip is inserted into the cam splicer (*see* **Fig. 3**). The transmission and reflection objectives also must be focused (*see* **Note 7**). The transmission objective is manually adjusted in X, Y, and Z (focus) with the translation knobs. The reflection objective is focused by manual rotation of the lens.

3.3. Sample Imaging

An NSOM image is composed of both topographic and optical information. A topographic image is first taken, which helps to set up the scan parameters and to identify the surface features (*see* **Note 8**). Finally, the combined image topographic and optical scan is taken (*see* **Notes 9**,**10**). The topographic image is almost identical to noncontact mode of the AFM technique. For topographic scanning, the probe is brought into feedback. Once the tip is in the feedback position and the probe can track the topography of the sample at a near-field range, NSOM imaging can be performed. A block diagram of the experimental setup is shown in **Fig. 4**.

3.4. Parameters for Topographical and NSOM Images

First the drive frequency for each probe is set to the resonant frequency of the tuning fork so that the magnitude of the tuning fork vibration can be maximized by adjusting the drive frequency. Typically, a frequency range between 90 and 100 kHz is selected for the tuning folk. After zooming in on the peak,

it is necessary for the amplitude to be about 5 V, which corresponds to approx 30 nA on the internal sensor signal. Fine-tuning the noncontact controls is then performed with the aim of having the drive amplitude as low as possible while maintaining the internal sensor signal constant and the root mean square noise (RMS) <0.1.

The tip is brought into the feedback via two approaches: "automatic" and "manual" feedback. The automatic feedback approach uses the automatic features programmed into the SPMlab software to lower the tip toward the sample surface. The manual feedback approach is more difficult and requires more care while lowering the tip to a distance within a few microns above the surface. The initial P-I-D setting for the topographical imaging was as follows: P = 1, I = 0.05, D = 0. The set point value was –64 nA (*see* **Note 11**). Once the tip is in feedback with the surface, the P-I-D parameters were adjusted to optimize the scan (*see* **Note 12**).

Because the laser light heats and expands the tip, some adjustments have to be made to the P-I-D settings before taking the NSOM images. In addition, the tuning fork frequency has to be rechecked. Once the P-I-D settings are optimized, NSOM images can be obtained (*see* **Note 13**).

3.5. Results and Discussion

As previously shown in reviews by Dunn ***(21)*** and Deckert ***(23)***, NSOM has emerged as a powerful tool for biological applications. The high resolution has enabled the study of functional molecular complexes ranging from chromosomes to membrane domains. To establish the usefulness of NSOM for imaging biological molecules, we wanted to investigate colocalization of proteins and their effects on chemotherapeutic drugs within the substructure of cells and cellular organelles. A phenomenon called MDR, which results from the overexpression of drug transporter proteins that belong to an ATP-binding cassette family of proteins, is the focus of our study.

P-gp and multidrug resistance protein-1 (MRP-1) are the two main proteins that are thought to be responsible for the extrusion of cytotoxic natural product amphipathic drugs from cancer cells. Clearly, the resistance of tumor cells to chemotherapeutic drugs has been a major clinical problem, and the pharmacological reversal of the function of the MDR transporter proteins is a significant area of interest. These proteins are assumed to be located in the plasma membrane ***(24,25)***; however, studies have demonstrated their location in other cellular organelles such as the endoplasmic reticulum ***(26,27)***. Although numerous factors have been associated with the development of MDR, studies largely support the role of an energy-dependent pump system in either extruding or excluding chemotherapeutic drugs from cells ***(28–30)***. Initial NSOM experiments to validate our system were performed on tumor cells (MTLN3) transfected with GFPs. The proteins are expressed in vivo and therefore can serve as

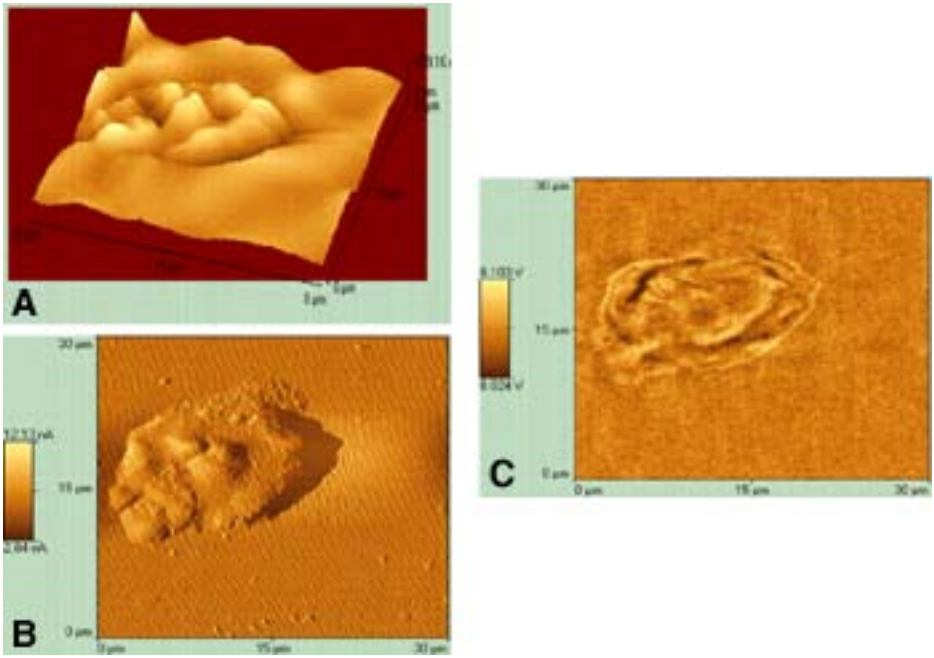

Fig. 5. MTLN3 tumor cells expressing GFP fusion proteins: **(A)** topography; **(B)** feedback internal signal; **(C)** fluorescence.

an indicator of internal structures and function within the cells. Previous studies have allowed visualization of the distribution of cell-surface EGF receptor (EGFR) in CHO cells that were stably transfected with a fusion construct of the EGFR and GFP. **Figure 5** shows topography, feedback internal signal, and fluorescence images of the MTLN3 tumor cells expressing the GFP fusion proteins. From these NSOM images, one can observe a homogeneous distribution of the protein in the cytoplasmic compartment of the cells.

Because of the superior resolution of NSOM, single-molecule studies have been carried out in which several hundred molecules per square micrometer can be observed. The level of sensitivity and accuracy has been proven to be far superior than for the far-field methods. Therefore, NSOM is an ideal technique for allowing independent observations of molecules at physiologically relevant packing densities. Additionally, the level of detail and sensitivity of NSOM allows colocalization studies in cases in which unprecedented information with high accuracy is required. We therefore chose to apply NSOM to study subcellular localization and the activity of MDR transport proteins. In this chapter, we do not show the specific locality of the proteins; nonethe-

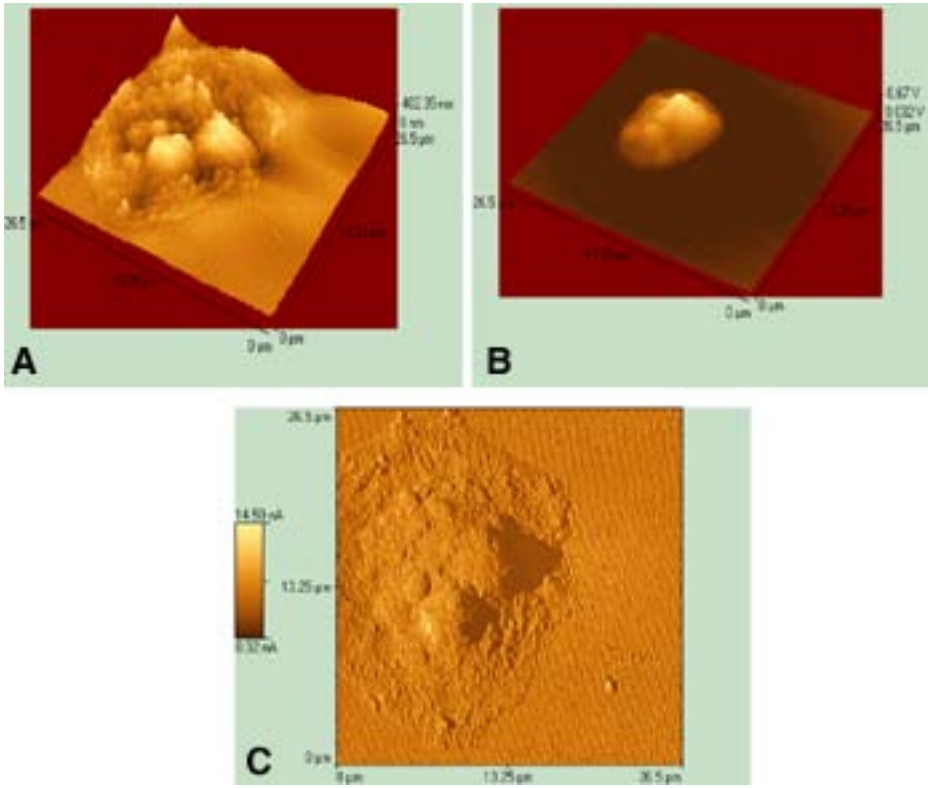

Fig. 6. NSOM image of CHO cells incubated with 5 μ*M* DOX: **(A)** topography; **(B)** fluorescence; **(C)** feedback internal signal.

less, we do demonstrate their effect on the localization of agents (drug and inhibitor) that interact with the proteins. Generally, MRP-1 and P-gp proteins are considered to be cell-surface localized and mediate drug resistance by lowering the total intracellular drug concentration ***(31,32)***. Several groups have tried to explain this MDR phenomenon and the mechanism of action using different models such as the energy-dependent pump system ***(30,33)***, but the localization of both proteins and the mechanism of action remain to be resolved.

To study the effect of MRP-1 transporters on the localization and accumulation of the anthracycline DOX and on yellow-green fluorescent FluoSpheres (data not shown), we used CHO and J774 cells (data not shown) that slightly expressed these proteins. The cells were incubated with 5 μ*M* DOX for 2 h at 37°C. They were then rinsed and fixed before imaging. **Figure 6** shows the topography and fluorescence images of CHO cells incubated with DOX. The fluorescence image clearly demonstrates nuclear localization of DOX.

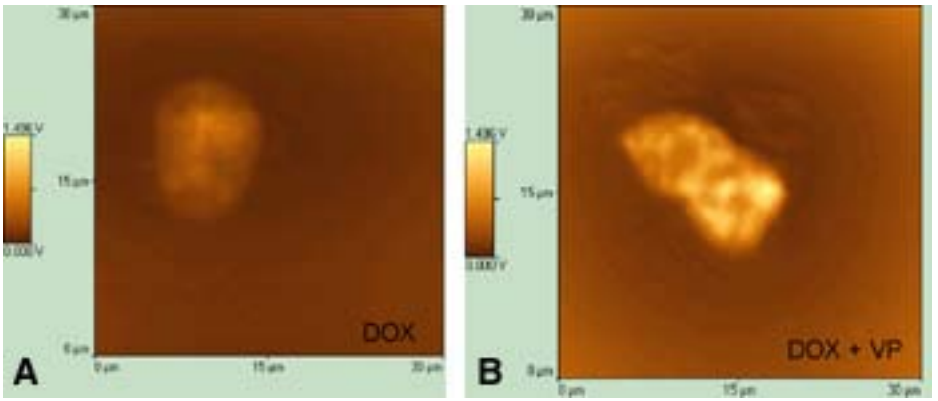

Fig. 7. NSOM images of CHO cells incubated with **(A)** 5 μ*M* DOX and **(B)** 5 μ*M* DOX + 5 μ*M* verapamil.

From the results in **Fig. 7**, we expected to see a high intracellular accumulation of drugs in cells that do not overly express the MDR transport proteins. However, suffice it to say that even cells that have not been exposed or transfected with these proteins do show some type of resistance. We demonstrated this phenomenon by inhibiting the function of the P-gp and MRP-1 proteins using an MDR reverser, verapamil. Interestingly, we observed that the addition of verapamil to CHO cells increased the cytotoxicity of DOX by fourfold. This kind of information clearly indicates that other factors (protein substrates) may also be associated with the drug resistance.

NSOM images of CHO cells that were incubated with only 5 μ*M* DOX and with both 5 μ*M* each of verapamil and DOX for 2 h at 37°C are shown in **Fig. 7**. Similar studies with cells transfected with MDR transporter proteins have been obtained ***(27,33)***. Conversely, the cells used in our study were normal CHO cells; thus, one would expect to observe little or no effect on the drug accumulation process. However, the results obtained with the CHO cells indicated that even normal cells may express these proteins at a level significant enough to efflux drugs from the cellular compartments. Therefore, the concentration and localization of multi-drug resistance proteins plays a vital role in the drug accumulation process. Using a highly sensitive technique with a high resolution such as NSOM provides unprecedented details on the effects of these MDR proteins. NSOM has therefore demonstrated that even in cases in which there is a low concentration of proteins, significant information can be obtained. Further studies are being conducted to localize the specific proteins and their activity in normal and tumor cells.

4. Notes

1. The fixed cells should be as flat as possible (<500 nm in height) so that the tip does not get out of feedback or become damaged.
2. To avoid damage to the piezo scanners, do not apply excessive force to the scanning stage.
3. To avoid damaging the piezo scanners, be careful not to touch the stage with the head.
4. To avoid damage to the probe and sample, handle the head with care, paying particular attention to the probe and probe mount on the bottom. Whenever the head is removed from the microscope stage, use the tip "up" button on the data acquisition tool bar to raise the tip a safe distance away from the sample. When placing the head on the stage, or when carefully setting it down on a table or other flat surface, turn the Z-height thumbscrews one full turn clockwise. Whenever the head is lowered using the Z motor or thumbscrews, watch the image on the video monitor to make sure that the probe does not crash into the sample or stage.
5. Because the probe is extremely fragile, handle it with care.
6. The NSOM probe is a fiber with one end tapered. Extra care is necessary while stripping off the cladding and cleaving the fiber.
7. First, the reflection objective should be used to locate the tip with the help of a camera. Second, the probe needs to be brought to the surface as close as possible, and the laser light coming out of the probe must be located using the transmission objective after turning off all the lights.
8. Once the probe is brought to feedback, the environment must be vibration free. Do not walk, open, or close the door; closing the door or walking by or touching the experimental setup table easily breaks the probe.
9. Exposure to light can damage the PMT. Thus, the light on the Aurora-2 must be off to prevent damage before the scan begins.
10. A sudden, dramatic increase in NSOM signal indicates a break in the tip, and the PMT voltage must immediately be lowered to prevent damage to the PMT.
11. Coupling the laser light into the probe is critical to obtain the optimum laser light. Do not couple the laser while the tip is in feedback.
12. The P-I-D setting should be low (especially the integral) so that the tip does not jump as it approaches the sample.
13. For the best topographic imaging, the P-I-D setting for each new tip has to be optimized.

Acknowledgments

This work was sponsored by the Office of Biological and Environmental Research, US Department of Energy, under contract DE-AC05-00OR22725 with UT-Battelle, LLC; and by the Laboratory Directed Research and Development Program (Advanced Plasmonics Sensor project) at Oak Ridge National Laboratory. M. Wabuyele and M. Culha are also supported by an appointment to the Oak Ridge National Laboratory Postdoctoral Research Associates Program, administered jointly by the Oak Ridge National Laboratory and Oak Ridge Institute for Science and Education.

References

1 Abbe, E. (1873) Beitrage zur Theorie des Mikroskops und der mikroskopischen Wahrnehmung. *Arch. Mikrosc. Anat. Entwicklungsmech*. **9,** 413–468.

2 Synge, E. H. (1928) A suggested method for extending microscopic resolution into the ultra-microscopic region. *Philos. Mag*. **6,** 356–362.

3 Ash, E. A. and Nicholls, G. (1972) Super-resolution aperture scanning microscope. *Nature (Lond.)* **237,** 510–512.

4. Mrksich, M. and Whitesides, G. M. (1995) Patterning self-assembled monolayers using microcontact printing: a new technology for biosensors. *Trends Biotechnol.* **13,** 228–235.

5 Lange, F., Cambi, A., Huijbens, R., de Bakker, B., Rensen, W., Garcia-Parajo, M., van Hulst, N., and Figdor, G. C. (2001) Cell biology beyond the diffraction limit: near-field scanning optical microscopy. *J. Cell Sci.* **114,** 4153–4160.

6. Betzig, E. and Chichester, R. (1993) Single molecules observed by near-field scanning optical microscopy. *Science* **262,** 1422–1424.

7 Zenobi, R. and Deckert, V. (2000) Scanning near-field optical microscopy and spectroscopy as a tool for chemical analysis. *Angew. Chem. Int. Ed.* **39,** 1747–1757.

8 Doyle, R. T., Szulzcewski, M. J., and Haydon, P. G. (2001) Extraction of near-field fluorescence from composite signals to provide high resolution images of glial cells. *Biophys. J.* **80,** 2477–2482.

9 Moers, M. H., Kalle, W. H., Ruiter, A. G., Wiegant, J. C., Raap, A. K., Greve, J., de Grooth, B. G., and Van Hulst, N. F. (1996) Fluorescence in situ hybridization on human metaphase chromosomes detected by near-field scanning optical microscopy. *J. Microsc.* **182,** 40–45.

10 Garcia-Parajo, M. F., Veerman, J. A., Segers-Nolten, A. G., and Van Hulst, N. F. (1998) Near-field optical and shear-force microscopy of single fluorophores and DNA molecules. *Ultramicroscopy* **71,** 311–319.

11 Garcia-Parajo, M. F., Veerman, J. A., Segers-Nolten, G. M. J., de Grooth, B. G., Greve, J., and van Hulst, N. F. (1999) Visualising individual green fluorescent proteins with a near field optical microscope. *Cytometry* **36,** 239–246.

12. Kirsch, A. K., Meyer, C. K., and Jovin, T. M. (1997) Shear force imaging of DNA in a near-field scanning optical microscope. *J. Microsc.* **185,** 396–401.

13 Betzig, E., Chichester, R. J., Lanni, F., and Taylor, D. L. (1993) Near-field fluorescence imaging of skeletal actin. *Bioimaging* **1,** 129–135.

14 Enderle, T., Ha, T., Ogletree, D. F., Chemla, D. S., Magowan, C., and Weiss, S. (1997) Membrane specific mapping and colocalization of malarial and host skeletal proteins in the *Plasmodium falciparum* infected erythrocyte by dual-color near-field scanning optical microscopy. *Proc. Natl. Acad. Sci. USA* **94,** 520–525.

15 Nagy, P., Jenei, A., Kirsch, A. K., Szollosi, J., Damjanovich, S., and Jovin, T. M. (1999) Activation-dependent clustering of the erbB2 receptor tyrosine kinase

detected by scanning near-field optical microscopy. *J. Cell. Sci.* **112,** 1733–1741.
16. Deckert, V., Zeisel, D., Zenobi, R., and Vo-Dinh, T. (1998) Near-field surface enhanced Raman imaging of dye-labeled DNA with 100-nm resolution. *Anal. Chem.* **70,** 2646–2650.
17 Garcia-Parajo, M. F., Veerman, J. A., van Noort, S. J. T., de Grooth, B. G., Greve, J., and van Hulst, N. F. (1998) Near-field optical microscopy for DNA studies at the single molecular level. *Bioimaging* **6,** 43–53.
18. Emory, S. R. and Nie, S. (1997) Near-field surface-enhanced Raman spectroscopy on single silver nanoparticles. *Anal. Chem.* **69,** 2631–2635.
19. Zeisel, D., Deckert, V., Zenobi, R., and Vo-Dinh, T. (1998) Near-field surface-enhanced Raman spectroscopy of dye molecules adsorbed on silver island films. *Chem. Phys. Lett.* **283,** 381–385.
20. Schmalenberg, K. E., Thompson, D. M., Buettner, H. M., Uhrich, K. E., and Garfias, L. F. (2002) In situ stepwise surface analysis of micropatterned glass substrates in liquids using functional near-field scanning optical microscopy. *Langmuir* **18,** 8593–8600.
21 Dunn, R. C. (1999) Near-field scanning optical microscopy. *Chem. Rev.* **99,** 2891–2927.
22. Merrit, M. V., Mrksich, M., and Whitesides, G. M. (1997) Using self-assembled monolayers to study the interactions of man-made materials with proteins, in *Principles of Tissue Engineering* (Lanza, R. P., Langer, R., and Chick, W., eds.), R. G. Landes Company, Austin, TX, pp. 211–223.
23. Deckert, V. (2003) Near-field imaging in biological and biomedical applications, in *Biomedical Photonics Handbook* (Vo-Dinh, T., ed.), CRC Press, Boca Raton, FL, pp. 12–19.
24 Zaman, G. J. R., Flens, M. J., van Leusden, M. R., et al. (1994) The human multidrug resistance-associated protein MRP is a plasma membrane drug-efflux pump. *Proc. Natl. Acad. Sci. USA* **91,** 8822–8826.
25. Shapiro, A. B., Fox, K., Lam, P., and Ling, V. (1999) Stimulation of P-glycoprotein-mediated drug transport by prazosin and progesterone: evidence for a third drug-binding site. *Eur. J Biochem.* **3,** 841–850.
26 Krisnamachary, N. and Center, M. S. (1993) The MRP gene associated with a non-P-glycoprotein multidrug resistance encodes a 190-kDa membrane bound glycoprotein. *Cancer Res.* **53,** 3658–3661.
27 Barrand, M. A., Heppell-Parton, A. C., Wright, K. A., Rabbits, P. H., and Twentyman, P. R. (1994) A 190-kilodalton protein overexpressed in non-P-glycoprotein-containing multidrug-resistant cells and its relationship to the MRP gene. *J. Natl. Cancer Inst.* **86,** 110–117.
28 Borst, P. (1999) Multidrug resistance: a solvable problem? *Ann. Oncol.* **10,** 162–164.
29 Sharom, F. J. (1997) The P-glycoprotein efflux pump: how does it transport drugs? *J. Membr. Biol.* **160,** 161–175.
30 Sauna, E. Z., Smith, M. M., Muller, M., Kerr, M. K., and Ambudkar, V. S. (2001) The mechanism of action of multidrug-resistance-linked p-glycoprotein. *J. Bioenerg. Biomembr.* **33,** 481–491.

31 Stride, D. B., Cole, C. P. S., and Deeley, G. R. (1999) Localization of substrate specificity domain in the multidrug resistance proteins. *J. Biol. Chem.* **274,** 22,877–22,883.
32. Hamilton, K. O., Topp, E., Makagiansar, I., Siahaan, T., Yazdanian, M., and Audus, L. K. (2001) Multidrug resistance-associated protein-1 functional activity in Calu-3 cells. *J. Pharmacol. Exp. Ther.* **3,** 1199–1205.
33. Chen, Y., Pant, A. C., and Simon, M. S. (2001) P-Glycoprotein does not reduce substrate concentration from the extracellular leaflet of the plasma membrane in living cells. *Cancer Res.* **61,** 7763–7769.